Overcoming Severe XEDS Peak Overlaps with the AEM

Scott D. Walck

South Bay Technology, Inc.
San Clemente, CA 92673
walck@southbaytech.com

Of all the analytical techniques in electron microscopy, X-ray energy dispersive spectroscopy (XEDS) is perhaps the most useful. It provides a quick identification of the elements and even with semi-quantitative methods; a reasonable composition can be obtained. However, in the scanning electron microscopy (SEM), there are materials systems in which severe peak overlaps of heavier elements *L* and *M* lines cannot be easily deconvolved with lighter elements' *K* lines. In addition, without a sufficient overvoltage in the SEM, even identification of the heavier elements can be difficult. In the analytical electron microscope (AEM), there is always sufficient overvoltage to excite all of the elements' *K*-lines. However, all of the *K*-lines might not be able to be detected with commercially available instruments. This is illustrated in Fig.1 where the maximum energy of the detector system might be set to 10, 20, or 40 keV. Careful examination of Fig. 1 would indicate that in the AEM, the problems associated with elemental identification of the elements can be overcome because of the presence of the higher energy X-rays, particularly if the range of 40 keV is used. However, there still exists the problem of a lighter element's *K* peak overlapping with a lower energy *L* or *M* X-ray peak from a heavier element and thus preventing the integrated peak intensity for that line to be extracted. For quantification, the heavier element would use the higher energy X-ray peak, but the lighter element's *K* intensity is needed for the complete quantification.

Fig. 1 Periodic Table showing the highest available X-ray lines with detector system set at A) 10 keV, B) 20 keV, and C) 40 keV. The solid colors indicate which elements would fluoresce the K, L, and M lines in these energy ranges.

While working at the Materials Directorate at Wright Patterson Air Force Base, I was involved with the characterization of advanced tribological thin films used as solid lubricants. One material that looked promising as an adaptive lubricant was a pulsed laser deposited PbO-MoS$_2$.[1] An adaptive lubricant is one that adapts it properties to the environmental parameters such as temperature and atmosphere to provide continuous lubrication. The PLD PbO-MoS$_2$ system held the possibility of offering the low temperature lubricant phase, MoS$_2$, and the high temperature lubricant phases PbO or PbMoO$_4$. In addition, different phases and microstructures would develop in the thin film depending on the processing that it was given. Identifying these phases proved to be difficult because of the peak overlaps of the S-*K*α, Mo-*L*α, and Pb-*M*α lines as shown in Fig. 2. We were interested in the partitioning of these elements in the different phases that formed. The process

that I used with the AEM will be discussed below.

What I would like to do in this article is to show how it is possible using an AEM to overcome the peak overlaps of a light element when the heavier elements' higher energy X-rays are present. The process relies on two assumptions that are fairly reasonable. The first is that the partitioning of the X-ray lines from a particular element is independent of the matrix, *i.e.* the composition and crystalline structure of the sample. For heavier elements that generate *L* and *M* lines, this is a very good assumption. To the analyst, what this means is that the ratio of the integrated peak intensities of a higher energy line to a lower energy line is constant. The second assumption is that the sample and all standards used in the analysis satisfy the thin film criteria for X-ray microanalysis. Following Williams[2] and Zaluzec[3], the thin film criteria is given as $\chi \rho t \leq 0.1$, where ρ is the density of the sample, t is the thickness of the sample, and $\chi = \mu/\rho \csc \psi$ and where
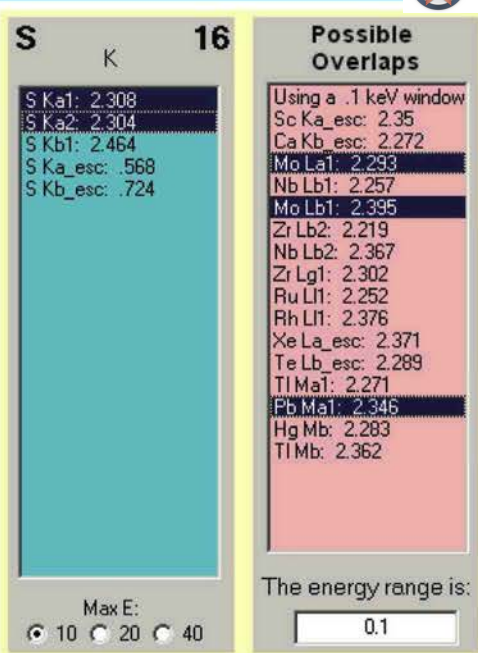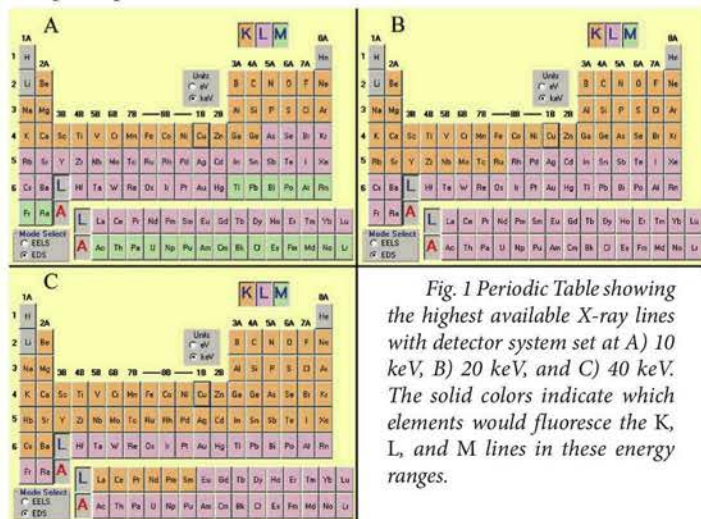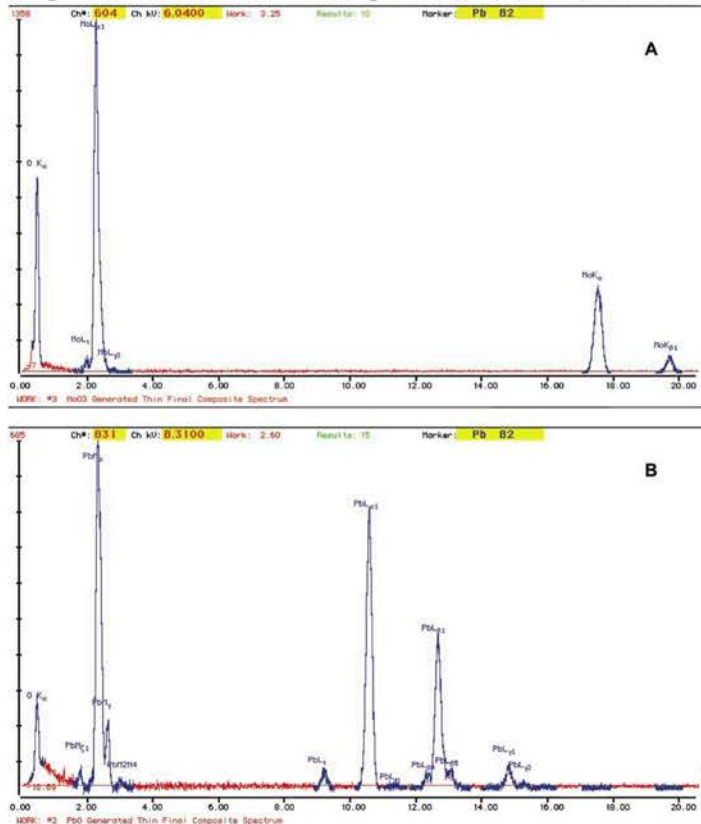

Fig. 2 Peak overlaps for a PbO-MoS$_2$ system. The highlighted X-ray lines are the overlapped peaks centered on the S-*K*α line.

Fig. 3 XEDS spectra from A) MoO$_3$ and B) PbO that show the relative peak heights in a JEOL 2000FX TEM.

Table 1
Intensities, Ratio, K-factors, and Analysis Results

Determination of Ratios

Mo					Pb			
I(Mo L)	I(Mo Ka)	R(Mo-L/K)	I(O K)		I(Pb M)	I(Pb La)	R(Pb-M/L)	I(O K)
19237	7048	2.73	7968		23636	17905	1.32	4959

Determination of K factors (Mo,S) and (Mo,O)

I(Mo Ka)	I(Mo L+ S K)	I(Mo L)$_{calc}$	I(S K)	k(MoS)	k(MoO)$_{W/Abs}$	k(MoO)	k(OS)$_{W/Abs}$	k(OS)$_{cor}$
10425	63810	28454	35356	5.07	2.26	2.81	2.24	1.81

Determination of K factors (Pb,S) and (Pb,O)

I(Pb La)	I(Pb M+ S K)	I(Pb M)calc	I(S K)	k(PbS)	k(PbO)$_{W/Abs}$	k(PbO)$_{cor}$	k(OS)$_{W/Abs}$	k(OS)$_{cor}$
16991	35717	22429	13288	5.05	3.57	4.79	1.42	1.06

Stoichiometric PbO-MoS2 Intensity Data

	I(MoKa)	Calc I(MoLa)	I(PbLa)	Calc I(PbMa)	I(Oka)	I(PbMa,MoLa,Ska)	S by Sub
	9827	26822	20054	26473	6400	86920	33625

Stoichiometric PbO-MoS2 Concentration Ratios C-L Analyzed from Generated Spectrum

C(Pb)/C(Mo)	C(Pb)/C(S)	C(Pb)/C(O)	ACF corrected	C(Mo)/C(S)	C(Mo)/C(O)	ACF corrected	C(O)/C(S)	ACF corrected
2.036	3.014	15.006	11.740	1.481	4.309	3.371	0.201	0.253

Stoichiometric PbO-MoS2 Concentration Ratios from Formula

2.160	3.240	12.881		1.497	5.952		0.336	

Errors (Relative to Formula Generated Values)

5.7%	7.0%	16.5%	8.9%	1.1%	27.6%	43.4%	40.2%	24.6%

μ/ρ is the mass absorption coefficient, and ψ is the takeoff angle. In the case of a wedge sample, csc ψ would be replaced with the appropriate geometric terms, as discussed by Zaluzec. This assumption is usually the most critical for the X-rays overlapped with the light element K-line. For the analyst, it means that the sample and standards do not significantly absorb the X-rays. This is important because any absorption of the X-rays will change the ratio of the higher energy line to the lower energy line. This assumption is entirely dependent on the method of sample preparation of the sample and standards. However, with the
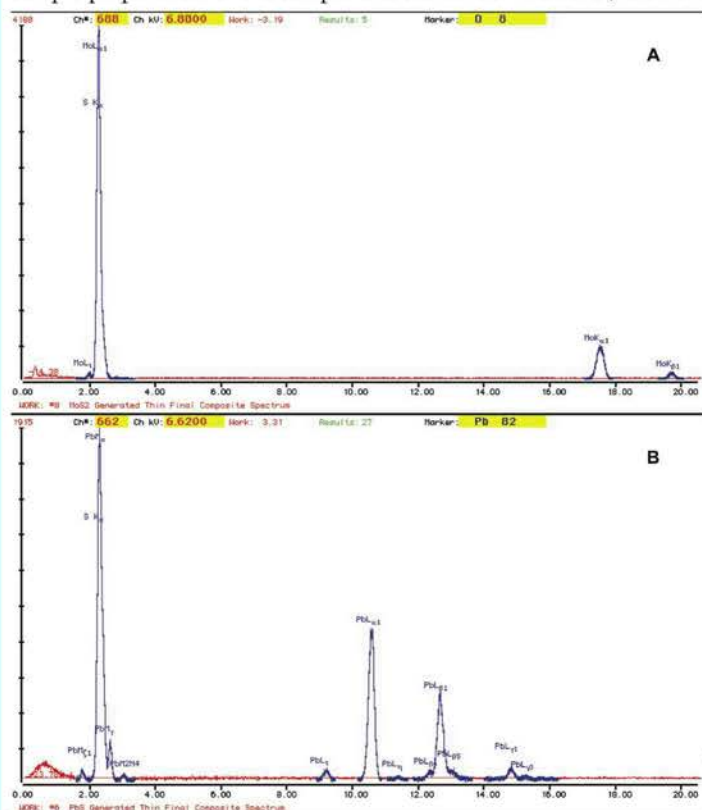
Fig. 4 XEDS spectra from A) MoS$_2$ and B) PbS used to determine the Cliff-Lorimer k-factors.

techniques available today for TEM sample preparation, it will be assumed that suitable samples can be prepared. (Is that a third assumption? If it is, then call me and we will talk about sample preparation.)

I will use the PLD PbO-MoS$_2$ system to illustrate the procedure. However, I no longer have the original data, so I modeled them using the DTSA (DeskTop Spectrum Analyzer) software available from NIST.[4] The modeling of the standards and unknown are done here only to illustrate the process. For the work reported in the paper, the XEDS detector was not capable of detecting oxygen. What was reported was the ratio of the concentrations of the elements. In the paper, when there was a single phase present or the electron beam was spread out over a larger area, the values agreed fairly well with X-ray photoelectron spectroscopy (XPS) results, which report an average of the thin film composition. For this exercise, I will include the oxygen since it is only a simulation and no one will believe the results for it anyway. The AEM system modeled was a JEOL 2000FX TEM with a Kevex Quantum detector. The parameters used in the modeling were 200 kV for accelerating voltage, 0.150 nA for the beam current, and 300 s live time. All of the samples were considered to be uniform, parallel-sided, 50 nm-thick thin films.

The first step in the process that is required is to determine the ratio of the higher energy line to the lower energy line. For lack of a better name, I will call this the elemental intensity ratio. For the same reasons that it is better to determine Cliff-Lorimer k-factors experimentally because of variations in TEM/XEDS systems, the elemental intensity ratios should be experimentally determined instead of accepting published values. For this system, it was easier to grind the Pb and Mo oxide and sulfide powders because I had them on hand. Only areas of the samples that showed kinematical convergent beam electron disks in the 200 keV instruments were used and strongly diffracting conditions were avoided. Fig. 3 shows the modeled X-ray spectra from MoO$_3$ and PbO 50 nm thick standards from DTSA. The integrated peak intensities and elemental intensity ratio values are given in Table 1. In the table, the ratio is found to be the Intensity of the lower energy line to the higher energy line, e.g. $R_{Mo-L/K} = I_{Mo-L\alpha} / I_{Mo-K\alpha}$.

The next step is to determine the k-factors for the Cliff-Lorimer analysis. For this step, PbS and MoS$_2$ were used as the standards. Fig. 4 shows the modeled X-ray spectra from these materials. The overlapped S intensities were found after subtracting the Pb-$M\alpha$ and the Mo-$L\alpha$ lines from their convoluted peaks, respectively. To do this, the intensity of the Mo-$L\alpha$ and the Pb-$M\alpha$ lines are found by using the ratio value found in the first step and then subtracting the calculated intensity from the convoluted overlapped peak. For example, the intensity of the S-K line from MoS$_2$ is given as $I_{S-K} = I_{(Mo-L + S-K)} - R_{Mo-L/K} * I_{Mo-K\alpha}$. After this is done, the k-factors were determined. These results are also given in Table 1.

Fig. 5 Stoichometric PbO-MoS₂ as an unknown.
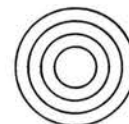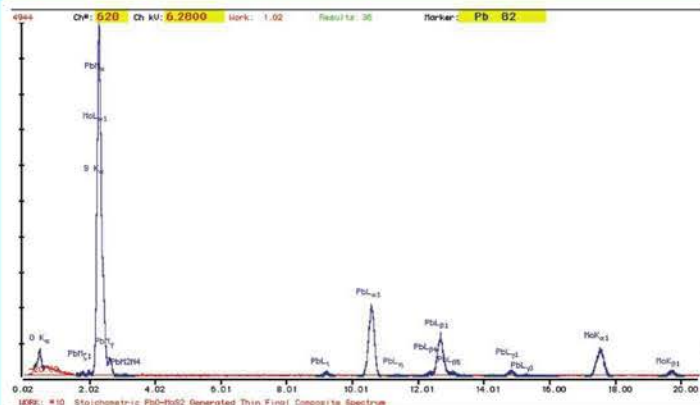
Now that the *k*-factors and elemental intensity ratios have been determined, the unknown can be acquired and analyzed. Fig. 5 shows the modeled spectrum from a stoichiometric PbO-MoS₂ film. For the case of the S-*K* line, the calculated Pb-*Mα* and the Mo-*Lα* were subtracted from the convoluted peak. The intensities and concentration ratios for the generated sample are given in Table 1. In the original study, the coatings were deposited by pulsed laser deposition. Because of this, the samples were oxygen deficient. They were also sulfur deficient, but this varied with the substrate temperature during deposition. We were primarily interested in the ratio of the elements from the deposition process. As mentioned above, we did not have a light element detector. As the results in Table 1 suggest, even at this artificial thickness of 50 nm, there would have been tremendous absorption of the O-*K* lines with this material system and with the standards.

One thing that should jump out from performing these steps is the proliferation of the accumulation of experimental errors, just on the basis of counting statistics alone. The *k*-factors and the elemental intensity ratios are formed from the ratio of two intensities and then the calculated intensity uses the product of that value with another intensity which is then subtracted from yet another intensity; then the concentration is calculated by applying the *k*-factors to two more intensities. (That sentence was as dizzying to write as it is to read.) Realistically, it means that pain must be taken to acquire many spectra from the first two steps in the process in order to minimize the contribution of experimental errors from the intensity ratio values and the *k*-factors, since those are formed from ratio of intensities whose errors are determined by counting statistics. Further, the error associated with each ratio would be found by the quadrature summation of the individual errors. I would recommend that the reader review the sections on experimental errors in any of the X-ray analysis sections of texts on electron microscopy. As riddled as this process is with the accumulation of errors in order to get the integrated peak intensity of the S-*K* line, it did provide a result that I was comfortable in reporting because it was the only method to obtain the partitioning of the elements in the samples with multiple phases and a fine microstructure. The models that were used here are ideal cases for the standards and the unknown. Overcoming the triple overlap of Pb, Mo, and S was an extreme example of this process. However, using it to overcome a double overlap, such as was done for the MoS₂ and PbS samples should be relatively simple in comparison. ∎

References

1. *Characterization of Pulsed Laser Deposited PbO/MoS₂ by Transmission Electron Microscopy*, S. D. Walck, M. S. Donley, J. S. Zabinski, and V. J. Dyhouse, J. Mat. Res., **9** (1), pp. 236-45, 1994.
2. D. B. Williams, Practical Analytical Electron Microscopy in Materials Science, Philips Electronic Instruments, Inc., Mahwah, NJ, 1984.
3. *Beginner's Guide to X-Ray Analysis in an Analytical Electron Microscope: Part 2 - Quantification Using Absorption and Fluorescence Corrections*, N. J. Zaluzec, EMSA Bulletin, **14**, (2), pp. 61-72, 1984.
4. See the website, http://www.cstl.nist.gov/div837/Division/outputs/DTSA/DTSA.htm, for a complete description of DTSA.